

## Dynamics of Individual Atomic Kinks during Crystal Dissolution

O. M. Magnussen and M. R. Vogt

*Abteilung Oberflächenchemie und Katalyse, Universität Ulm, 89069 Ulm, Germany*

(Received 1 March 2000)

The dynamics of kink motion via atom removal/deposition as a fundamental step in dissolution/crystallization of solids have become directly accessible by a novel scanning tunneling microscopy technique. Results obtained for the electrochemical dissolution of Cu(100) in HCl solution show pronounced local dissolution/redeposition fluctuations at the individual kinks even at the onset of Cu dissolution with average kink propagation and reaction rates in the range  $10^3$  and  $10^5$  atoms  $s^{-1}$ , respectively. These experiments allow one to directly measure the central kinetic properties of this electrochemical reaction.

PACS numbers: 82.45.+z, 83.70.Gp

Numerous chemical, biological, geological, and technological processes involve the dissolution or growth of solid crystals immersed in solution. It was suggested more than 70 years ago that the fundamental step in such dissolution/crystallization processes is the detachment/attachment of the basic building blocks of the crystal, e.g., atoms, ions, or molecules, at kinks in steps on the crystal surface [1]. In that picture both the kinetics of the dissolution/crystallization reactions as well as the equilibrium shape and morphology of crystals are determined by the rate of these processes [2]. Unfortunately, these rates are not accessible from macroscopic kinetic data, since the kink density is difficult to measure and usually depends in a complex manner on the surface morphology as well as on under-/supersaturation [3]. These problems could be avoided, however, if dissolution or growth at individual kink sites is determined directly by measurements on an atomic scale. The possibility of such measurements is demonstrated by dynamic *in situ* scanning tunneling microscopy (STM) observations of the electrochemical dissolution of Cu(100) in hydrochloric acid solution.

This reaction, which is also of technological importance for copper corrosion, etching, and electrorefinement, is especially well suited for these experiments from a number of experimental reasons: First, the dissolution rates can be sensitively controlled by the electrode potential. According to electrochemical measurements, Cu is dissolved in HCl solution as  $CuCl_2^-$ , involving the formation of a  $Cl_{ads}$  intermediate species, and the reaction exhibits quasi-Tafel behavior, i.e., an exponential potential dependence, at low dissolution rates (see Refs. [4,5], and references therein). Second, in the dissolution regime the Cu surface is covered by an ordered Cl adlayer with a  $c(2 \times 2)$  structure, which induces a pronounced faceting of the Cu steps (Fig. 1), resulting in straight, stable steps along the  $\{001\}$  directions with a very low kink density [6,7]. Third, the microscopic mechanism of the Cu dissolution process was studied extensively, showing that Cu(100) dissolution in HCl proceeds via removal of the primitive surface unit cells, i.e.,  $(\sqrt{2} \times \sqrt{2})R45^\circ$  units containing two Cu and an adsorbed Cl atom, at kinks in the  $\{001\}$ -oriented steps [illustrated schematically in Fig. 1(b)] [7]. As a result,

these kinks propagate along the steps (from left to right in Fig. 1) during the dissolution process.

The direct observation of kink motion by *in situ* STM is generally hampered by the high rate of this process, exceeding the maximum STM image acquisition rate (typically a few seconds) by orders of magnitude even at the very onset of Cu dissolution [7]. Much higher time resolution can be obtained if the STM scan is restricted to one dimension (“*x-t* scans”), which has been used extensively for the study of step fluctuations under equilibrium conditions both in ultrahigh vacuum and in electrochemical environment [8]. This method, however, measures only changes in the step positions resulting from kink migration,

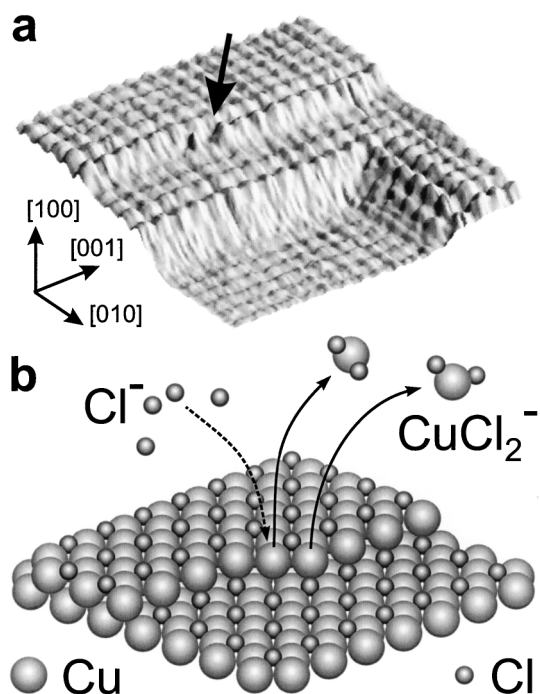


FIG. 1. Surface morphology of Cu(100) in HCl solution. (a) High-resolution *in situ* STM image ( $50 \times 50 \text{ \AA}^2$ ) showing the  $c(2 \times 2)$ -Cl adlattice as well as steps and kink sites (see arrow). (b) Model of the  $c(2 \times 2)$ -covered surface illustrating the mechanism of electrochemical dissolution via removal of  $(\sqrt{2} \times \sqrt{2})R45^\circ$  units at kink sites.

but does not allow one to directly observe the kink motion. In particular, the kink dynamics under nonequilibrium conditions, as is the case for dissolution or growth processes, cannot be studied by this method, since such processes are dominated by the net unidirectional migration of kinks along the steps. In the following we present the first results by a novel scanning technique, developed in our group, which includes the advantages of both scan types, namely, the high time resolution of the line scan technique and the direct observation of kink migration afforded by the recording of complete STM images.

Experiments were performed in a homebuilt STM in the constant current mode using W tips coated with Apiezon wax and a tip bias of typically  $-100$  mV.  $0.01M$  HCl prepared from suprapure HCl (Merck) and ultrapure water (milli-Q) was used as electrolyte. Potentials are referred against the saturated calomel electrode (SCE). Before each measurement, the Cu(100) sample was electrochemically polished for 10 s in 66% orthophosphoric acid (Merck, p.a.) at 2.4 V versus a Pt counterelectrode, rinsed with ultrapure water, and then immersed into the electrolyte at a potential in the range  $-0.45$  to  $-0.15$  V [7].

The method used to measure the kink motion is illustrated in Figs. 2(a) and 2(b). In that technique we record STM scan lines across an approximately perpendicular running step alternately at two locations ( $y_1$  and  $y_2$ ), separated by a distance  $\Delta y$ . At each location the passing of a kink manifests as a distinct change  $\Delta x$  in the step position along  $x$  by one or two (see below)  $(\sqrt{2} \times \sqrt{2})R45^\circ$  unit cell widths. Because of the low kink density and the consequently large separation of the kinks along the steps [see also Fig. 2(c)], the positional changes at  $y_1$  and  $y_2$  can be easily correlated, with the time difference  $\Delta t$  corresponding to the propagation time of the kink from  $y_1$  to  $y_2$ . This method of determining the average velocity of a single kink, which we call time-of-walk (TOW) measurements, is principally similar to the time-of-flight method used for measurements of the velocity of free particles.

Examples showing characteristic dissolution events are presented in Figs. 2(b) (raw data) and 2(c) [extracted step positions  $x(t)$  at  $y_1$  and  $y_2$ ]. The widths  $\Delta x$  of the abrupt positional changes associated with passing kinks are  $3.6$  Å (“single row” events) or  $7.2$  Å (“double row” events), with probabilities of 76% and 24%, respectively. The normalized distribution of kink propagation times  $N(\Delta t)/N_0$  for the majority kink species, i.e., for events where only the outermost row of  $(\sqrt{2} \times \sqrt{2})R45^\circ$  unit cells is dissolved, is presented in Fig. 3 for two potentials in the regime of low dissolution rates. Since  $N(\Delta t)/N_0$  was within the statistical error independent of the height of the steps (typically monatomic or two layers high), all single row events were used for the distributions displayed in Fig. 3. As can be seen in the figure, the average time required for kinks to travel the  $306$  Å from  $y_1$  to  $y_2$  is in the range of 50–200 ms, corresponding to dissolution rates of the order of  $10^{-3}$  s per  $(\sqrt{2} \times \sqrt{2})R45^\circ$  unit. A significant fraction

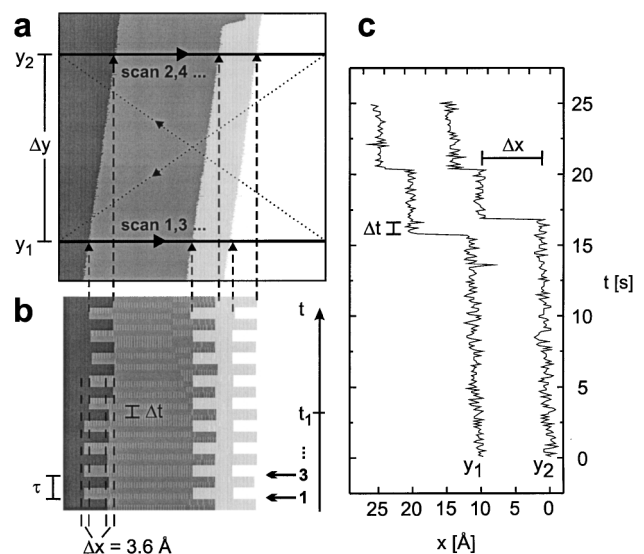


FIG. 2. Quantitative measurements of kink propagation velocities during Cu(100) dissolution in  $0.01M$  HCl by the TOW method. (a) An *in situ* STM image ( $170 \times 450$  Å<sup>2</sup>) recorded at  $-0.25$  V prior to the experiment, solid (recorded scan lines) and dotted (backscan) lines illustrate the path of the scanning tip during one TOW cycle. For clarity, each terrace is colored by a single color. (b) Small part of the TOW data, recorded after a potential step to  $-0.14$  V at positions  $y_1$  and  $y_2$  ( $\Delta y = 306$  Å; time per TOW cycle  $\tau = 100$  ms). At time  $t_1$  a kink in the leftmost step with a width of  $\Delta x = 3.6$  Å, i.e., one  $(\sqrt{2} \times \sqrt{2})R45^\circ$  unit, passes through  $y_1$  and  $y_2$ , whereas no positional changes occur at the other steps. (c) Step positions  $x(t)$  at  $y_1$  and  $y_2$ , extracted from similar TOW experiments and showing the passing of a kink with a width of single ( $t = 20.5$  s) and double ( $t = 16$  s)  $(\sqrt{2} \times \sqrt{2})R45^\circ$  units, respectively.

of the kinks, however, travels considerably slower, resulting in a broad tail in  $N(\Delta t)/N_0$ . We explain this distribution by strong positional fluctuations of the kinks along the steps caused by competing dissolution and redeposition processes. Such parallel dissolution and growth are expected from macroscopic electrochemical measurements and are the base for the exchange current density, one of the central kinetic parameters of electrochemical reactions.

For a quantitative evaluation we use a simple statistical model, assuming that dissolution and redeposition at kinks occur stochastically, with the probabilities for the removal/growth of one  $(\sqrt{2} \times \sqrt{2})R45^\circ$  unit at each kink site given by the constant (potential-dependent) dissolution and redeposition rates  $k_a$  and  $k_c$ , respectively. Close to equilibrium the (measured) average kink propagation rate  $\Delta k = k_a - k_c$  is considerably lower than the average reaction rates at kink sites  $\bar{k} = k_a + k_c$ , and the motion of the kinks along the steps is described by a one-dimensional random walk with a slight preference towards dissolution ( $k_a > k_c$ ). This model provides the most simple description of the (nonequilibrium) dynamics of kink motion, which explicitly accounts for positional fluctuations due to random dissolution/redeposition processes. The relative frequency  $N(\Delta t)/N_0$ , for which a time  $\Delta t$  is measured for

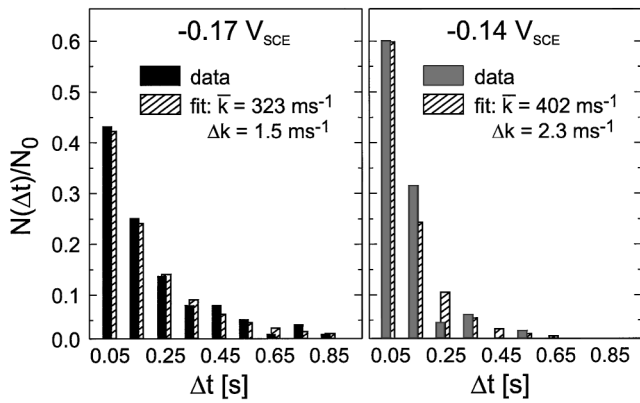


FIG. 3. Normalized distribution  $N(\Delta t)/N_0$  of the kink propagation times  $\Delta t$  for  $-0.17$  and  $-0.14$  V ( $\Delta y = 306$  Å). The striped columns are the results of fits to the statistical model (data columns correspond to  $i = 0-8$  TOW cycles passed in the interval  $\Delta t$ ). The relative errors in the average reaction rates at kinks sites  $\bar{k} = k_a + k_c$  and in the average kink propagation rate  $\Delta k = k_a - k_c$  are 24% and 35%, respectively.

a kink migrating from  $y_1$  to  $y_2$ , is within this model given by the probability  $P(\Delta t, \Delta y')$  of finding a kink after time  $\Delta t$  at a position  $\Delta y'$  [measured in  $(\sqrt{2} \times \sqrt{2})R45^\circ$  units, i.e.,  $\Delta y' \equiv \Delta y/(3.6 \text{ Å})$ ] farther down the step, convoluted by instrumental functions  $g_i(\Delta t)$ , which take into account the finite time resolution of the TOW experiment. In a continuum approximation  $P(\Delta t, \Delta y')$  is given by

$$\frac{d}{d\Delta t} P(\Delta y', \Delta t) = \frac{1}{2} \bar{k} \frac{d^2}{d\Delta y'^2} P(\Delta y', \Delta t) - \Delta k \frac{d}{d\Delta y'} P(\Delta y', \Delta t),$$

where the first term on the right-hand side of the equation corresponds to (symmetric) one-dimensional diffusion and the second term describes the net propagation of the kinks [9]. This is solved by the probability distribution function

$$P(\Delta t, \Delta y') = \frac{\Delta k}{\sqrt{2\pi\bar{k}\Delta t}} \exp\left(-\frac{(\Delta y' - \Delta k\Delta t)^2}{2\bar{k}\Delta t}\right).$$

Each of the (discrete) points of the measured distribution  $N(\Delta t)/N_0$  is obtained by convolution of  $P(\Delta t, \Delta y')$  by sawtooth-shaped instrumental functions  $g_i(\Delta t)$  with  $g_i(\Delta t) = [1 - |\Delta t/\tau - (i + \frac{1}{2})|] \tau^{-1}$  for  $(i - \frac{1}{2})\tau < \Delta t < (i + \frac{1}{2})\tau$ ,  $g_0(\Delta t) = \tau^{-1}$  for  $\Delta t < \tau/2$ , and  $g_i(\Delta t) = 0$  otherwise, where  $i$  corresponds to the number of TOW cycles passing between the change in step position at  $y_1$  and at  $y_2$  (i.e., during the propagation of the kink). The only adjustable parameters in this model are  $\bar{k}$  and  $\Delta k$ .

Fits of the experimental data sets and the corresponding parameters are included in Fig. 3. In these fits we have neglected the fact that, due to the two possible phase relationships of the Cl adlattice on the upper and lower Cu terrace, two types of steps with kinks of strongly different reactivity exist [7]. It is assumed that dissolution proceeds

predominantly at the more reactive sites, i.e., that only one of the two different types of kinks contributes significantly to the TOW data. Very recently, this assumption was directly confirmed in *in situ* video-STM observations by our group [10]. As can be seen in Fig. 3, the simple two parameter model provides a good description of the measured  $N(\Delta t)/N_0$  data [11]. Although the errors in  $\bar{k}$  and  $\Delta k$  are considerable due to the still limited time resolution, it is clear that the reaction rate at kinks is about 2 orders of magnitude larger than the average rate of kink propagation, i.e.,  $k_a$  and  $k_c$  differ by less than 1%. In addition, with increasing potential the kink propagation rate  $\Delta k$  and the reaction rate  $\bar{k}$  increase. The latter implies that not only the dissolution but also the redeposition rate increases, which can be attributed to the increasing  $\text{CuCl}_2^-$  concentration in the near surface region. These results directly demonstrate that each kink simultaneously acts as an active site for both the dissolution and the reverse deposition reaction and provides the first direct quantitative data for the microscopic rates of these atomic-scale processes, namely, kink propagation rates in the range  $10^3$  atoms  $\text{s}^{-1}$  and reaction rates of the order of  $10^5$  atoms  $\text{s}^{-1}$ .

The more rare double row events cannot be explained solely by the successive propagation of two independent single row kinks, which follow each other within a time interval smaller than the experimental resolution  $\tau$ . First, the positional changes occur almost exclusively in one scan line at both locations  $y_1$  and  $y_2$ , i.e., a splitting into two single row events at one of the locations is almost never observed. Second, the motion of the double row kinks is much slower [see, e.g., Fig. 2(c)] with about 3 times larger average propagation times  $\Delta t$  than for the single row events. Hence, we tentatively ascribe these events to a collective removal of two parallel  $(\sqrt{2} \times \sqrt{2})R45^\circ$  rows, a mechanism not conceived in previous models of crystal dissolution. In addition, from correlation of the direction of the kink motion (“single” and “double” row events) with the surrounding surface topography, it could be inferred that at least 90% of the kinks nucleate at the outer corners of the terraces.

Finally, the approximate macroscopic dissolution rate can be assessed from the microscopic data using the average kink propagation rate and an estimate of the average kink density obtained from the *in situ* STM observations. The average spacing of kinks along the steps is given by the average time difference between the successive dissolution events in the TOW measurements (about 40 s at  $-0.17$  V) multiplied by  $\Delta k \cdot 3.6$  Å. Together with the average step distance found in the STM images ( $\approx 100$  Å) and the dissolution current per kink  $2e\Delta k$ , a kink density of  $5 \times 10^{-8} \text{ cm}^{-2}$  and a dissolution current density of  $0.2 \mu\text{A cm}^{-2}$  are calculated. This is in excellent agreement with the current of  $0.25 \mu\text{A cm}^{-2}$  measured in quasi-static electrochemical polarization curves on the same Cu(100) crystal at this potential, confirming the validity of the experimental concept proposed here.

Several challenges exist for future studies by the TOW method, the most significant of which is to increase the time resolution, i.e., to decrease  $\tau$ . Since the motion of the kinks can not be infinitely fast, the probability distribution  $P(\Delta t, \Delta y')$  must exhibit a peak, which in our model is at  $t_{\text{peak}} = \frac{1}{2}\Delta k^{-2}(\sqrt{\bar{k}^2 + 4\Delta k^2\Delta y'^2} - \bar{k})$ . The experimental resolution of this maximum in the distribution  $N(\Delta t)/N_0$ , which according to the fit results would require a  $\tau \leq 10$  ms, is of key importance for improving the fit quality. Furthermore, for a well-defined electrochemical kinetics the experiments should be performed in solutions containing defined concentrations of Cu ions, which will also allow one to study the reverse Cu deposition reaction. Again, this will require a much higher time resolution of the STM, since under these conditions the surface morphology is highly dynamic at all potentials. Very recently, we constructed a novel *in situ* video-STM, capable of operating at a factor-100 higher speed, which will make these experiments feasible [12]. In the long run this type of measurement should help bridge the gap between traditional macroscopic kinetic data and modern theories of ion transfer reactions [13], leading to a true atomic-scale understanding of the dynamics of dissolution and crystallization processes.

We gratefully acknowledge financial support for O.M.M. by the Deutsche Forschungsgemeinschaft and financial support for M.R.V. by the Max Buchner Forschungsstiftung. Furthermore, we thank R.J. Behm for valuable discussions.

---

[1] I.N. Stranski, Z. Phys. Chem. **136**, 259 (1928).

[2] E. Budevski, G. Staikov, and W. J. Lorenz, *Electrochemical Phase Formation and Growth* (VCH, Weinheim, 1996).

- [3] W. Allgaier and K.E. Heusler, J. Appl. Electrochem. **9**, 155 (1979).
- [4] W.H. Smyrl, in *Electrochemical Materials Science*, edited by J.O. Bockris, B.E. Conway, E. Yeager, and R.E. White (Plenum Press, New York, 1981), Vol. 4, p. 97.
- [5] H.P. Lee and K. Nobe, J. Electrochem. Soc. **133**, 2035 (1983).
- [6] D.W. Suggs and A.J. Bard, J. Phys. Chem. **99**, 8349 (1995).
- [7] M.R. Vogt, F. Möller, C.M. Schilz, O.M. Magnussen, and R.J. Behm, Surf. Sci. **367**, L33 (1996); M.R. Vogt, A. Lachenwitzer, O.M. Magnussen, and R.J. Behm, Surf. Sci. **399**, 49 (1998).
- [8] M. Giesen-Seibert, R. Jentjens, M. Poensgen, and H. Ibach, Phys. Rev. Lett. **71**, 3521 (1993); M. Giesen, M. Dietterle, D. Stapel, H. Ibach, and D.M. Kolb, Surf. Sci. **384**, 168 (1997).
- [9] This formulation of the kink propagation equation and the derived probability distribution is valid only if the kink position  $\Delta y'$  is measured in dimensionless  $(\sqrt{2} \times \sqrt{2})R45^\circ$  units. If the position is measured in units of length  $\Delta y$ ,  $\bar{k}$  and  $\Delta k$  have to be replaced in both equations by  $a^2\bar{k}$  and  $a\Delta k$ , where  $a = 3.6 \text{ \AA}$  is the length of one  $(\sqrt{2} \times \sqrt{2})R45^\circ$  unit cell.
- [10] L. Zitzler, B. Gleich, O.M. Magnussen, and R.J. Behm, *Electrochim. Acta* (to be published).
- [11] Models with contributions of two types of kinks (i.e., four free parameters), resulting in bimodal distributions, do not give reliable fits with the current quality of the data. The same holds true for other, more complex (and more realistic) models, e.g., models where the individual deposition/dissolution events are described not by constant rates but by probability distributions or where these events are not statistically independent.
- [12] L. Zitzler, B. Gleich, O.M. Magnussen, and R.J. Behm, *Proc. Electrochem. Soc.* (to be published).
- [13] M.T.M. Koper and W. Schmickler, in *Electrocatalysis*, edited by J. Lipkowski and P.N. Ross (Wiley-VCH, New York, 1998), p. 291.